


# Significant Enhancement of Near-Field Electromagnetic Heat Transfer in a Multilayer Structure through Multiple Surface-States Coupling

Hideo Iizuka<sup>1,\*</sup> and Shanhui Fan<sup>2,†</sup>

<sup>1</sup>*Toyota Research Institute of North America, Toyota Motor North America, Ann Arbor, Michigan 48105, USA*

<sup>2</sup>*Department of Electrical Engineering, Ginzton Laboratory, Stanford University, Stanford, California 94305, USA*

 (Received 4 October 2017; published 8 February 2018)

We show that near-field electromagnetic heat transfer between multilayer thermal bodies can be significantly enhanced by the contributions of surface states at multiple surfaces. As a demonstration, we show that when one of the materials forming the multilayer structure is described by the Drude model, and the other one is a vacuum, at the same gap spacing the resulting heat transfer can be up to 40 times higher as compared to that between two semi-infinite materials described by the same Drude model. Moreover, this system can exhibit a nonmonotonic dependency in its heat transfer coefficient as a function of the middle gap spacing. The enhancement effect in the system persists for realistic materials.

DOI: [10.1103/PhysRevLett.120.063901](https://doi.org/10.1103/PhysRevLett.120.063901)

Electromagnetic near-field heat transfer is of great importance in heat management at nanoscale since it exceeds the blackbody limit by several orders of magnitude [1–17]. In most configurations, one considers two semi-infinite dielectric or metal bodies separated by a vacuum gap [Fig. 1(a)]. The near-field heat transfer is then significantly enhanced due to the presence of the surface states at the body-vacuum interfaces. There has been a large amount of literature seeking to maximize such near-field heat transfer by controlling various material and structural parameters [18–41].

Since the dominant contribution to heat transfer arises from surface states, a natural idea for the enhancement is to use multiple surface states in the heat transfer. For example, one can consider the geometry shown in Fig. 1(c), where each body consists of multiple layers of alternating materials. The bodies are separated by a vacuum gap in the middle. In this case, there are certainly a lot more surfaces that can support surface states. Moreover, when the two materials have positive and negative dielectric constants, respectively, the resulting structure can homogenize to have a hyperbolic effective permittivity tensor. References [36–40] showed that near-field heat transfer can be enhanced between two *uniform* hyperbolic media. On the other hand, Miller *et al.* [41] analyzed a multilayer system as shown in Fig. 1(c) without using homogenization, and noted that the heat transfer is dominated by the contributions of the surfaces immediately adjacent to the vacuum gap. Intuitively, the spacing between the surfaces not immediately adjacent to the middle vacuum gap is large, and as a result, the states on these surfaces do not contribute to heat transfer significantly.

In this Letter, we reexamine the multilayer geometry as shown in Fig. 1(c). We point out that under the right condition, intermediate layers can facilitate the energy

transfer from surface states located away from the middle vacuum gap. As a result, one can in fact achieve significant enhancement of near-field heat transfer by having contributions from multiple interfaces. Similar to the conclusion of Ref. [41], this enhancement also cannot be accounted for by the effective medium model. As a demonstration, we

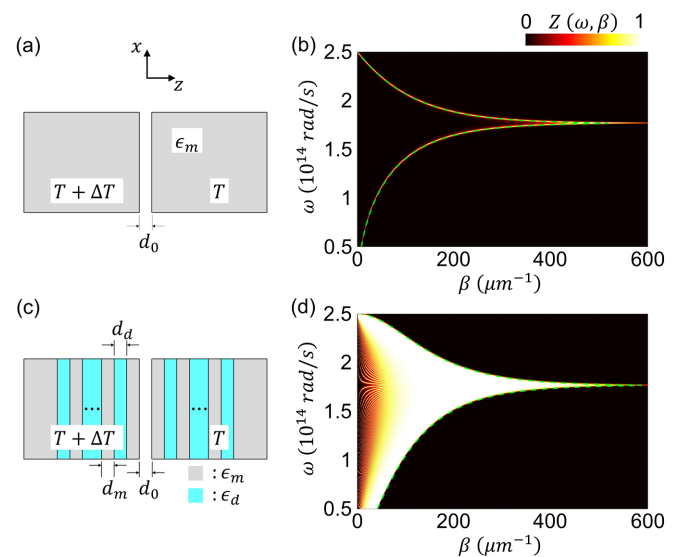


FIG. 1. Geometries and exchange functions of the bulk system [(a),(b)] and the multilayer system [(c),(d)]. The green dashed lines in (b) and (d) correspond to the dispersion curves as determined by Eqs. (5) and (4), respectively. For the metal with a dielectric constant  $\epsilon_m$ , we assume the Drude model in Eq. (1) with  $\epsilon_\infty = 1$ ,  $\omega_p = 2.5 \times 10^{14}$  rad/s, and  $\gamma = 1 \times 10^{12}$  rad/s. For the dielectric, we assume  $\epsilon_d = 1$ . Other parameters are  $d_0 = d_m = d_d = 10$  nm,  $T = 300$  K, and  $N = 80$  unit cells in each body. These parameters are used throughout the Letter unless otherwise mentioned.

show that when one of the materials forming the multilayer structure is described by the Drude model, and the other one is a vacuum, with the correct choice of the parameters for the Drude model, at the same gap spacing the resulting heat transfer can be more than 40 times higher as compared to that between two semi-infinite materials described by the same Drude model. We also show that the enhancement effect persists for realistic materials. Moreover, this system can exhibit a nonmonotonic dependency in its heat transfer coefficient as a function of the middle gap spacing. Prior to our work, there has not been any indication that such nonmonotonic behavior can occur in a planar geometry [1–5,9–13].

We start with a brief overview of the fluctuational electrodynamics for investigating electromagnetic heat transfer in the multilayer system [40] as shown in Fig. 1(c). For simplicity, we assume that the two bodies are mirror images of each other. Both are periodic. Each body consists of  $N$  unit cells. Each unit cell consists of a lossless dielectric layer with a permittivity  $\epsilon_d$ , and a lossy material layer, with its permittivity  $\epsilon_m$  described by the Drude model:

$$\epsilon_m(\omega) = \epsilon_\infty - \frac{\omega_p^2}{\omega(\omega + i\gamma)}. \quad (1)$$

In Eq. (1),  $\epsilon_\infty$ ,  $\omega_p$ , and  $\gamma$  are the permittivity at infinite frequency, the plasma frequency, and the damping rate, respectively. We refer to the material that is described by the Drude model as “metal” for the rest of the Letter. We maintain the two bodies at the temperatures of  $T + \Delta T$  and  $T$ , respectively. When the middle vacuum gap size  $d_0$  is smaller than the characteristic thermal wavelength,  $p$ -polarized evanescent waves dominantly contribute to the heat transfer and the heat transfer coefficient between the two bodies is given by [4]

$$h = \frac{\partial}{\partial T} \int_{k_0}^{\infty} \frac{\beta d\beta}{2\pi} \int_0^{\infty} \frac{d\omega}{2\pi} Z(\omega, \beta) \Theta(\omega, T), \quad (2)$$

where the exchange function  $Z(\omega, \beta)$  ( $0 \leq Z \leq 1$ ) is

$$Z(\omega, \beta) = \frac{4\{\text{Im}[r(\omega, \beta)]\}^2 e^{-2\kappa_0 d_0}}{|1 - r(\omega, \beta)|^2 e^{-2\kappa_0 d_0}}, \quad (3)$$

$r(\omega, \beta)$  is the Fresnel reflection coefficient of the  $p$ -polarized evanescent waves from the vacuum to one of the bodies,  $\Theta(\omega, T) = \hbar\omega / (e^{\hbar\omega/k_B T} - 1)$  is the mean thermal energy of a single optical mode at the frequency  $\omega$ ,  $\hbar$  and  $k_B$  are the reduced Planck constant and the Boltzmann constant, respectively.  $\kappa_0 = \sqrt{\beta^2 - k_0^2}$  ( $k_0 < \beta$ ) is the wave number component normal to the layers in vacuum, where  $k_0$  is the free-space wave number, and  $\beta$  is the lateral wave number to the surfaces.

As a concrete example, we set the thicknesses of layers to be equal to the width of the vacuum gap, i.e.,  $d_m = d_d = d_0 = 10$  nm, and the dielectric layers are set to be a vacuum with  $\epsilon_d = 1$ . For metal layers, we choose the parameters in the Drude model to be  $\epsilon_\infty = 1$ ,  $\omega_p = 2.5 \times 10^{14}$  rad/s, and  $\gamma = 1 \times 10^{12}$  rad/s. This choice of parameters results in a surface plasmon frequency similar to the surface phonon-polariton frequency of the interface between silicon carbide (SiC) and vacuum. We select  $N = 80$  unit cells in each body and set a temperature of  $T = 300$  K. These parameters are used throughout the Letter unless otherwise mentioned.

The exchange function  $Z(\omega, \beta)$  in the multilayer system of Fig. 1(c) is plotted in Fig. 1(d). Remarkably, we see that there exists an *area* of near-unity value for  $Z(\omega, \beta)$  in the  $\omega$ - $\beta$  phase space due to the contributions of surface states at multiple surfaces. The outer circumference of the near-unity area agrees well with the dispersion equation:

$$\left(\frac{\epsilon_m}{\kappa_m} + \frac{\epsilon_d}{\kappa_d}\right)^2 \cosh(\kappa_m d_m + \kappa_d d_d) - \left(\frac{\epsilon_m}{\kappa_m} - \frac{\epsilon_d}{\kappa_d}\right)^2 \cosh(\kappa_m d_m - \kappa_d d_d) + \frac{4\epsilon_m \epsilon_d}{\kappa_m \kappa_d} = 0, \quad (4)$$

where  $\kappa_{m,d} = \sqrt{\beta^2 - \epsilon_{m,d} k_0^2}$ . For a given  $\beta$ , the solution of Eq. (4) for  $\omega$  corresponds to minimum and maximum eigenfrequencies for an infinitely periodic structure with the same unit cell as the finite structure we consider here. [The derivation of Eq. (4) can be found in Supplemental Material [42]] In contrast, in the  $\omega$ - $\beta$  phase space, for heat transfer between two semi-infinite metal regions,  $Z(\omega, \beta)$  has two near-unity *lines* [Fig. 1(b)], which agrees with the dispersion equation of the coupled surface states at the metal-vacuum interfaces [4]:

$$\left(\frac{\epsilon_m}{\kappa_m} + \frac{1}{\kappa_0}\right)^2 e^{\kappa_0 d_0} - \left(\frac{\epsilon_m}{\kappa_m} - \frac{1}{\kappa_0}\right)^2 e^{-\kappa_0 d_0} = 0. \quad (5)$$

The presence of an area where  $Z(\omega, \beta)$  is near-unity indicates that many states are contributing to the heat transfer. Therefore, the surfaces that are located far away from the middle gap must also contribute significantly to the heat transfer. To illustrate the mechanism in which the surfaces far away from the middle gap can contribute to heat transfer, we consider the structure of Fig. 2(a), where four lossless metal layers described by the lossless Drude model are placed in the vacuum gap between two semi-infinite lossy metal bodies described by the same Drude model as above. There are ten surfaces that have the same resonance frequency of  $\omega_0 = \omega_p / \sqrt{2}$ . In the regime of  $\beta \gg k_0$ , we have approximately the same wave number  $\kappa_m = \kappa_d = \kappa_0 = \beta$ , i.e., the same coupling rates between neighboring surface states in the same spaces of  $d_m = d_d = d_0 = 10$  nm, and the damping rate becomes

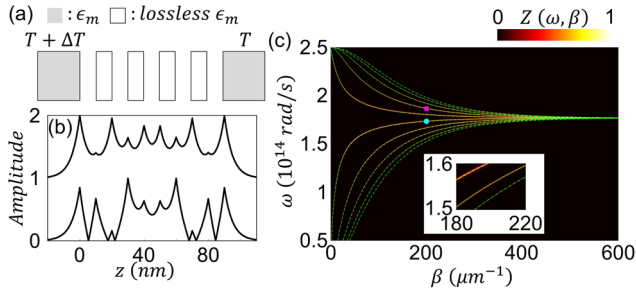


FIG. 2. (a) Two semi-infinite metal bodies separated by a vacuum gap size of 90 nm and four lossless metal layers are placed between them. (b) Mode profiles at  $(\omega, \beta)$  that are indicated by the cyan circle (top profile) and the pink square (bottom profile) in (c), respectively. (c) Exchange function for the structure, with ten dispersion curves of the structure superimposed shown as red and green curves.

$\gamma/2$  [44]. In such a system, ten modes [two modes of them are presented in Figs. 2(b)] contribute to the heat transfer significantly. As a result,  $Z(\omega, \beta)$  has ten peaks of near-unity at a constant  $\beta$  [Fig. 2(c)]. The dispersion curves of these modes can be obtained using a similar transfer matrix method as outlined in Supplemental Material [42]. On the other hand, in the absence of the lossless metal layers, the two surfaces of the semi-infinite metal bodies only couple weakly and the heat transfer is significantly decreased (Supplemental Material [42]). Comparing this example with the structure in Fig. 1, we see that, in the structure of Fig. 1, the interfaces away from the middle gap provide additional surface states, which serve as “relay” that enables surfaces farther away from the middle gap to contribute to the heat transfer. This mechanism of using surface states as relay in the near field underlies Pendry’s superlens proposal [45], and has been applied in the control of near-field heat transfer in a three-body system [46]. Here, we show that this relay mechanism can drastically enhance the heat transfer in a multilayer system.

In the near-field heat transfer between two semi-infinite metal bodies with a fixed gap size, there is an optimal damping rate that maximizes the heat transfer coefficient (Fig. 3, pink dash-dotted line). By the fluctuation-dissipation theorem, the strength of the fluctuating dipoles that provide the source of the thermal radiation is proportional to the imaginary part of the dielectric constant. Thus, when the damping rate approaches zero there is no heat transfer between the states on the two surfaces. On the other hand, at too large a damping rate the effect of surface resonance diminishes, which reduces the magnitude of the heat transfer coefficient.

In contrast, for the multilayer system, the dependency of the heat transfer coefficient  $h$  on the damping rate  $\gamma$  reaches maximum at the small  $\gamma$  limit (Fig. 3, blue solid line). In obtaining the results for the multilayer system, for each value of  $\gamma$ , we increase the number of layers  $N$  until  $h$  no longer changes with  $N$ . (See Supplemental Material [42]

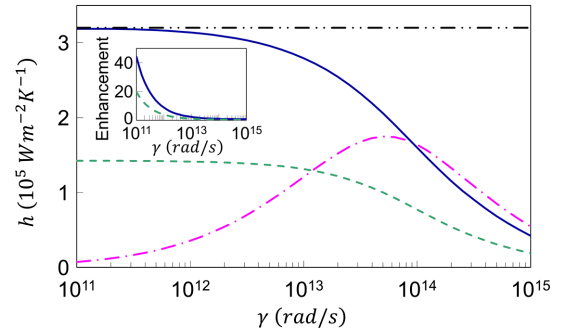


FIG. 3. Heat transfer coefficients  $h$  as a function of the damping rate  $\gamma$ . The blue solid, pink dash-dotted, or green dashed line corresponds to the case of multilayer system, bulk system, or effective medium model system, respectively. The geometries and all parameters are the same as in Fig. 1 except for  $\gamma$  and the number of unit cells  $N$  in the multilayer system, where for each value of  $\gamma$ ,  $N$  is increased until  $h$  no longer changes with  $N$ . The horizontal black dash-double-dotted line represents  $h$  in the small  $\gamma$  limit [Eq. (6)]. The inset shows the enhancement factor of the multilayer system with respect to the bulk system as a function of  $\gamma$ .

for discussions of  $h$  as a function of  $\gamma$  for a fixed  $N$ .) Intuitively, as  $\gamma$  decreases, the contributions from individual surface states decrease. However, at the same time, the number of surfaces that contribute to the heat transfer increases as  $\gamma$  decreases. These two competing trends balance each other at the low  $\gamma$  limit.

Based on the intuitive argument above, the heat transfer coefficient for the multilayer system at the small  $\gamma$  limit can be computed by an analytic model. At this limit, all surface states contribute. The heat transfer coefficient can then be approximated as

$$h = \frac{\partial}{\partial T} \int_{k_0}^{\infty} \frac{\beta d\beta}{2\pi} \int_{\omega_L(\beta)}^{\omega_H(\beta)} \frac{d\omega}{2\pi} \Theta(\omega, T), \quad (6)$$

where  $\omega_L(\beta)$  and  $\omega_H(\beta)$  are obtained from Eq. (4), and correspond to the lower and upper bounds of the eigenfrequencies of all states in the multilayer system at a given  $\beta$ . In the regime where  $\beta \gg k_0$ ,  $\omega_L(\beta) = \omega_0 \{1 - [(\epsilon_d - 1) \sinh^2(\beta d_0/2) + \epsilon_d] / [(\epsilon_\infty + \epsilon_d) \sinh^2(\beta d_0/2) + \epsilon_d]\}^{1/2}$  and  $\omega_H(\beta) = \omega_0 \{1 + [(1 - \epsilon_d) \cosh^2(\beta d_0/2) + \epsilon_d] / [(\epsilon_\infty + \epsilon_d) \cosh^2(\beta d_0/2) - \epsilon_d]\}^{1/2}$ . We see that Eq. (6) agrees excellently with the numerical results in the low  $\gamma$  limit (Fig. 3).

In the inset of Fig. 3, we plot the ratio of heat transfer coefficient  $h$  between the multilayer system and the bulk system. For the same Drude model parameters, the multilayer system exhibits greatly enhanced  $h$ , especially in the regime of low  $\gamma$ , where the enhancement can be as high as 40-fold. Even when allowing  $\gamma$  to vary, the maximum  $h$  in the multilayer case, which occurs at the low  $\gamma$  regime, still exceeds the maximum in the bulk system by a factor of 2.

The results here indicate the significant potential of using a multilayer system for the enhancement of near-field heat transfer, especially in material systems where the material damping rate is below the optimal damping rate for semi-infinite systems.

In the multilayer system as considered here, the periodicity is far smaller as compared to the relevant thermal wavelength at the chosen temperature. Such a multilayer system is usually described by an effective medium model, where the parallel and perpendicular components of the permittivity, as defined with respect to the surface of the layers, are approximately given by  $\epsilon_{\parallel} = (\epsilon_m d_m + \epsilon_d d_d) / (d_m + d_d)$  and  $\epsilon_{\perp} = \epsilon_m \epsilon_d (d_m + d_d) / (\epsilon_m d_d + \epsilon_d d_m)$  [35]. For the parameters that we choose here, the effective medium model corresponds to a hyperbolic medium in the relevant thermal wavelength range. In Fig. 3, we also plot the heat transfer coefficient  $h$  as a function of damping rate  $\gamma$  for such an effective medium model. We see that  $h$  of the multilayer system significantly exceeds the prediction from the effective medium model. This is in contrast with the case considered in Ref. [41], where the heat transfer coefficient of the multilayer system falls below that of the effective medium model. Compared with the corresponding multilayer system, the exchange function of the effective medium model has far less contributions from the surface states (Supplemental Material [42]), which explains the discrepancy.

In Fig. 4, we plot the heat transfer coefficient  $h$  for the multilayer system as considered in Fig. 1, where we vary the middle gap size while keeping all other parameters fixed. We also compare the behavior of the multilayer layer system with that of the bulk system as described by the Drude model, and the effective medium model that corresponds to the multilayer system. For the bulk system,  $h$  exhibits the well-known  $1/d_0^2$  dependency. We see that the behavior of the multilayer system is similar to the bulk in the small  $d_0$  limit. For the multilayer system, the relay mechanism, as we discussed in Fig. 2, works best when  $d_0$

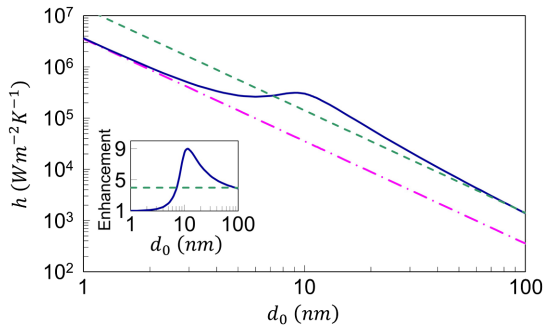


FIG. 4. Dependency of heat transfer coefficients  $h$  as a function of the size  $d_0$  of the middle vacuum gap, for the multilayer system (blue solid line), bulk system (pink dash-dotted line), and effective medium model system (green dashed line). The inset shows the enhancement ratio as a function of  $d_0$ .

is comparable to the layer thickness, similar to the optimal condition for the geometry that exhibits the superlens effect [45]. In the small  $d_0$  limit, the relay mechanism is no longer effective. The heat transfer is then dominated only by the surfaces immediately adjacent to the middle gap. And, therefore, the behavior of the multilayer system approaches that of the bulk. In the large  $d_0$  limit, the behavior of the multilayer system approaches that of the effective medium, where the heat transfer is mostly carried by waves with relatively small wave vector components parallel to the interface. Such waves, having a longer effective wavelength, are well described by the effective index model.

Remarkably, the multilayer system we consider can exhibit a nonmonotonic dependency of heat transfer on the middle gap size  $d_0$ . As we reduce  $d_0$  from 9 to 6 nm, the heat transfer actually *decreases* (Fig. 4). As  $d_0$  is reduced from 10 nm, which is the optimal middle gap size for the relay mechanism, the reduction of the contributions from surfaces away from the middle gap more than offsets the increase of the contributions from the surfaces adjacent to the middle gap, leading to the overall reduction of the heat transfer coefficient  $h$ . Such a nonmonotonic dependency of  $h$  on  $d_0$  has been previously observed numerically only in systems with somewhat unusual geometries, such as between a sphere and a plate with a hole in it [47], and has never been noted in a planar system before.

Up to now in this Letter, we have chosen the Drude model with arbitrary parameters in order to illustrate the rich physics in this system. In what follows, we show that one practically important aspect of our results, i.e., the significant enhancement in the heat transfer, persists in realistic structures. We choose SiC as the “metal” layer since it has a negative dielectric constant in the frequency range of interest, and is also commonly used in the study of near-field heat transfer. SiC has a permittivity  $\epsilon_m(\omega) = \epsilon_{\infty}(\omega_{LO}^2 - \omega^2 - i\gamma\omega) / (\omega_{TO}^2 - \omega^2 - i\gamma\omega)$ , with parameters of  $\epsilon_{\infty} = 6.7$ ,  $\omega_{LO} = 1.83 \times 10^{14}$  rad/s,  $\omega_{TO} = 1.49 \times 10^{14}$  rad/s, and  $\gamma = 8.97 \times 10^{11}$  rad/s [3]. As has been

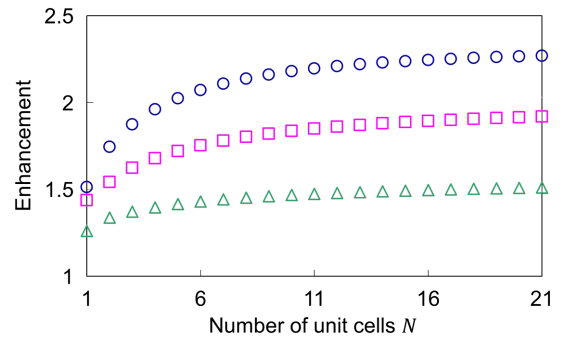


FIG. 5. Enhancement of heat transfer coefficients in the multilayer system [Fig. 1(c)] with respect to the bulk system [Fig. 1(a)] as a function of the number of unit cells. The “metal” layers correspond to SiC. The dielectric layers are vacuum (blue circles), dielectric with  $\epsilon_d = 2$  (pink squares), and dielectric with  $\epsilon_d = 4$  (green triangles).



noted in Ref. [48], SiC has a damping rate that is in fact less than optimal for maximizing near-field heat transfer. Therefore, from our discussions above in Fig. 3, the use of multilayer geometry is particularly beneficial to enhance heat transfer in systems based on SiC. In Fig. 5, we consider three different systems where the dielectric layers have  $\epsilon_d = 4, 2,$  and  $1,$  respectively, and we plot the heat transfer coefficient normalized against that of two semi-infinite SiC regions in each case as the number of unit cells varies. All three systems show significant enhancement against heat transfer between two semi-finite SiC regions. As  $\epsilon_d$  increases, heat transfer is decreased due to the mismatch of resonance frequencies between  $\omega_d = \omega_p/\sqrt{\epsilon_d+1}$  at interfaces within the thermal bodies and  $\omega_0 = \omega_p/\sqrt{2}$  at the interface of the middle vacuum gap and each of the SiC layers. Nevertheless, an enhancement factor of 2 is obtained when  $\epsilon_d = 2,$  which corresponds to materials such as barium fluoride and strontium fluoride. Therefore, significant enhancement can be observed with realistic materials. In addition, we can see significant enhancement even with  $N < 5.$  A large number of layers is not needed for the enhancement. The enhancement factor we observe here is significantly higher as compared to previous calculations assuming realistic material parameters. The improvement here arises primarily from our use of dielectric layers with low dielectric constants. When  $\epsilon_d = 4,$  we observe a decreased enhancement factor of 1.5, which is only slightly higher than what has been obtained in previous works, where the dielectric material is assumed to be silicon dioxide with  $\epsilon_d \approx 3.9$  [35–38,41] or germanium with  $\epsilon_d \approx 16$  [39,40].

In conclusion, we have shown that heat transfer in a multilayer system can be significantly enhanced by the contributions of surface states at multiple surfaces. The enhancement of heat transfer is most pronounced when the multilayer system consists of low-loss metal layers and low-permittivity dielectric layers. In addition, the multilayer system can exhibit a nonmonotonic dependency of the heat transfer on the middle gap spacing. The enhancement of heat transfer persists for realistic material systems. Our results provide analytical insights for heat transfer enhancement at nanoscale.

---

\*hideo.iizuka@toyota.com

†shanhui@stanford.edu

- [1] D. Polder and M. Van Hove, *Phys. Rev. B* **4**, 3303 (1971).
- [2] J. B. Pendry, *J. Phys. Condens. Matter* **11**, 6621 (1999).
- [3] K. Joulain, J.-P. Mulet, F. Marquier, R. Carminati, and J.-J. Greffet, *Surf. Sci. Rep.* **57**, 59 (2005).
- [4] S. Basu, Z. M. Zhang, and C. J. Fu, *Int. J. Energy Res.* **33**, 1203 (2009).
- [5] D. G. Cahill, P. V. Braun, G. Chen, D. R. Clarke, S. Fan, K. E. Goodson, P. Keblinski, W. P. King, G. D. Mahan, A. Majumdar, H. J. Maris, S. R. Phillpot, E. Pop, and L. Shi, *Appl. Phys. Rev.* **1**, 011305 (2014).
- [6] E. Rousseau, A. Siria, G. Jourdan, S. Volz, F. Comin, J. Chevrier, and J.-J. Greffet, *Nat. Photonics* **3**, 514 (2009).
- [7] S. Shen, A. Narayanaswamy, and G. Chen, *Nano Lett.* **9**, 2909 (2009).
- [8] K. Kim, B. Song, V. Fernandez-Hurtado, W. Lee, W. Jeong, L. Cui, D. Thompson, J. Feist, M. T. Homer Reid, F. J. Garcia-Vidal, J. C. Cuevas, E. Meyhofer, and P. Reddy, *Nature (London)* **528**, 387 (2015).
- [9] Lu Hu, A. Narayanaswamy, X. Chen, and G. Chen, *Appl. Phys. Lett.* **92**, 133106 (2008).
- [10] R. S. Ottens, V. Quetschke, S. Wise, A. A. Alemi, R. Lundock, G. Mueller, D. H. Reitze, D. B. Tanner, and B. F. Whiting, *Phys. Rev. Lett.* **107**, 014301 (2011).
- [11] R. St-Gelais, B. Guha, L. Zhu, S. Fan, and M. Lipson, *Nano Lett.* **14**, 6971 (2014).
- [12] K. Ito, A. Miura, H. Iizuka, and H. Toshiyoshi, *Appl. Phys. Lett.* **106**, 083504 (2015).
- [13] M. P. Bernardi, D. Milovich, and M. Francoeur, *Nat. Commun.* **7**, 12900 (2016).
- [14] A. Kittel, W. Muller-Hirsch, J. Parisi, S.-A. Biehs, D. Reddig, and M. Holthaus, *Phys. Rev. Lett.* **95**, 224301 (2005).
- [15] Y. De Wilde, F. Formanek, R. Carminati, B. Gralak, P.-A. Lemoine, K. Joulain, J.-P. Mulet, Y. Chen, and J.-J. Greffet, *Nature (London)* **444**, 740 (2006).
- [16] B. Guha, C. Otey, C. B. Poitras, S. Fan, and M. Lipson, *Nano Lett.* **12**, 4546 (2012).
- [17] K. Ito, K. Nishikawa, A. Miura, H. Toshiyoshi, and H. Iizuka, *Nano Lett.* **17**, 4347 (2017).
- [18] M. Francoeur, M. P. Menguc, and R. Vaillon, *Appl. Phys. Lett.* **93**, 043109 (2008).
- [19] P. Ben-Abdallah, K. Joulain, and A. Pryamikov, *Appl. Phys. Lett.* **96**, 143117 (2010).
- [20] S.-A. Biehs, P. Ben-Abdallah, F. S. S. Rosa, K. Joulain, and J.-J. Greffet, *Opt. Express* **19**, A1088 (2011).
- [21] A. W. Rodriguez, O. Ilic, P. Bermel, I. Celanovic, J. D. Joannopoulos, M. Soljacic, and S. G. Johnson, *Phys. Rev. Lett.* **107**, 114302 (2011).
- [22] R. Guerout, J. Lussange, F. S. S. Rosa, J.-P. Hugonin, D. A. R. Dalvit, J.-J. Greffet, A. Lambrecht, and S. Reynaud, *Phys. Rev. B* **85**, 180301(R) (2012).
- [23] J. Dai, S. A. Dyakov, and M. Yan, *Phys. Rev. B* **92**, 035419 (2015).
- [24] Y. Yang and L. Wang, *Phys. Rev. Lett.* **117**, 044301 (2016).
- [25] V. Fernandez-Hurtado, F. J. Garcia-Vidal, S. Fan, and J. C. Cuevas, *Phys. Rev. Lett.* **118**, 203901 (2017).
- [26] K. Joulain, J. Drevillon, and P. Ben-Abdallah, *Phys. Rev. B* **81**, 165119 (2010).
- [27] M. Francoeur, M. P. Menguc, and R. Vaillon, *Opt. Express* **19**, 18774 (2011).
- [28] S.-A. Biehs, and M. Tschikin, and P. Ben-Abdallah, *Phys. Rev. Lett.* **109**, 104301 (2012).
- [29] B. Liu and S. Shen, *Phys. Rev. B* **87**, 115403 (2013).
- [30] C. Simovski, S. Maslovski, I. Nefedov, and S. Tretyakov, *Opt. Express* **21**, 14988 (2013).
- [31] T. Ikeda, K. Ito, and H. Iizuka, *J. Appl. Phys.* **121**, 013106 (2017).

- [32] X. L. Liu, R. Z. Zhang, and Z. M. Zhang, *ACS Photonics* **1**, 785 (2014).
- [33] X. L. Liu and Z. M. Zhang, *Appl. Phys. Lett.* **107**, 143114 (2015).
- [34] K. Shi, F. Bao, and S. He, *ACS Photonics* **4**, 971 (2017).
- [35] S. Jin, M. Lim, S. S. Lee, and B. J. Lee, *Opt. Express* **24**, A635 (2016).
- [36] Y. Guo, C. L. Cortes, S. Molesky, and Z. Jacob, *Appl. Phys. Lett.* **101**, 131106 (2012).
- [37] Y. Guo and Z. Jacob, *Opt. Express* **21**, 15014 (2013).
- [38] S.-A. Biehs, M. Tschikin, R. Messina, and P. Ben-Abdallah, *Appl. Phys. Lett.* **102**, 131106 (2013).
- [39] T. J. Bright, X. L. Liu, and Z. M. Zhang, *Opt. Express* **22**, A1112 (2014).
- [40] S.-A. Biehs and P. Ben-Abdallah, *Z. Naturforsch. A* **72**, 115 (2017).
- [41] O. D. Miller, S. G. Johnson, and A. W. Rodriguez, *Phys. Rev. Lett.* **112**, 157402 (2014).
- [42] See Supplemental Material at <http://link.aps.org/supplemental/10.1103/PhysRevLett.120.063901> for the derivation of Eq. (4) and discussions of heat transfer exchanges in various systems, which includes Ref. [43].
- [43] P. Yeh, A. Yariv, and C.-S. Hong, *J. Opt. Soc. Am.* **67**, 423 (1977).
- [44] A. Raman, W. Shin, and S. Fan, *Phys. Rev. Lett.* **110**, 183901 (2013).
- [45] J. B. Pendry, *Phys. Rev. Lett.* **85**, 3966 (2000).
- [46] R. Messina, M. Antezza, and P. Ben-Abdallah, *Phys. Rev. Lett.* **109**, 244302 (2012).
- [47] A. W. Rodriguez, M. T. Homer Reid, J. Varela, J. D. Joannopoulos, F. Capasso, and S. G. Johnson, *Phys. Rev. Lett.* **110**, 014301 (2013).
- [48] H. Iizuka and S. Fan, *J. Appl. Phys.* **122**, 124306 (2017).